Hydrological Signatures Relating the Asian Summer Monsoon and ENSO

J. FASULLO AND P. J. WEBSTER

Program in Oceanic and Atmospheric Sciences, University of Colorado, Boulder, Colorado

(Manuscript received 10 December 2001, in final form 1 May 2002)

ABSTRACT

Using the NCEP–NCAR reanalysis for the 1950–2000 period, differences in the atmospheric hydrological cycle between the extremes of ENSO (i.e., La Niña minus El Niño) are examined. Zonal vertically integrated moisture transport (VIMT) across 100°E accounts for about half of the variability in net moisture convergence in the north Indian Ocean region between ENSO extremes when all ENSO events are considered. Changes in VIMT across 100°E are associated with large changes in the strength of the Pacific Ocean trade wind regime during ENSO. The bulk of the remaining VIMT anomalies are from the Arabian Sea and appear to be associated with sea level pressure variations in the northern and western parts of the Indian Ocean Basin. This initial analysis, therefore, suggests that the interaction between the monsoon and ENSO may be more complex than the direct modulation of VIMT by the Pacific Ocean trade winds alone.

The analysis is refined further by comparing the differences of the Indian and Pacific Ocean hydrological cycles between ENSO extremes when they occur concurrently with anomalous monsoons [ENSO–anomalous monsoon years (EAM)], and when the monsoon is normal [ENSO–normal monsoon years (ENM)]. For both EAM and ENM years, similar differences exist in VIMT across 100°E between ENSO extremes. However, major differences are noted in VIMT anomalies from the west and south into the north Indian Ocean region. Thus, the principal difference in moisture convergence in the north Indian Ocean between EAM and ENM years is associated primarily with VIMT anomalies in the western Indian Ocean region and not those in the eastern Indian or Pacific Oceans.

To test the hypothesis that Pacific Ocean SST anomalies occurring prior to the monsoon may be important in influencing the eventual nature of the monsoon, the analysis is extended backward to the spring period. While May SST differences in the Niño-3 region between ENSO extremes are found to be similar for both EAM and ENM years, VIMT differences in both the Indian Ocean and the central and western Pacific Oceans are significantly larger during EAM years than ENM years. May SST differences in the central subtropical Pacific Ocean are also significantly larger during EAM than ENM years. These results show that the anomalous SST gradient between the eastern equatorial and the central subtropical Pacific Ocean prior to the monsoon onset, together with its associated VIMTs anomalies, may be important factors in determining the degree of connection between monsoon and ENSO. In addition, the circulation in the Indian Ocean prior to and during the monsoon onset shares a strong association with the eventual intensity of the monsoon–ENSO coupling.

1. Introduction

The largest concentration of latent heating on the planet is spread across the warm pools of the Pacific and Indian Oceans and the South Asian continent during boreal summer (e.g., Rodwell and Hoskins 2001). Fluctuations in monsoon rains are also accompanied by large changes in atmospheric heating on the scale of south Asia. The scale and magnitude of these heating perturbations are such that they have the potential of influencing and responding to other modes of tropical variability such as the El Niño–Southern Oscillation (ENSO). However, the interaction of the monsoon with other large-scale climatological features is very complex and is therefore difficult to interpret. Early investigations of teleconnections with the monsoon region reveal a moderate correlation between anomalies in rainfall during June–July–August–September (JJAS) and sea surface temperatures (SST) in the eastern tropical Pacific Ocean on an interannual timescale of about −0.55 (e.g., Walker 1923; Barnett 1983; Shukla and Paolina 1983; Rasmusson and Carpenter 1983). The physical nature of a monsoon–ENSO teleconnection is often explained as an interaction between the Hadley circulation in the monsoon region with changes in moisture convergence driven by the trade winds and a perturbed Walker circulation during ENSO (e.g., Rasmusson and Carpenter 1983; Barnett 1983, 1984; Webster and Yang 1992; Ju and Slingo 1995; Lau and Bua 1998; Goswami 1998). According to these theories, the net result of the interaction is a reduction in moisture transport into south Asia during El Niño events and an enhancement of convergence during La Niña events (Sikka 1980; Pant and

Corresponding author address: Dr. J. Fasullo, Program in Oceanic and Atmospheric Sciences, University of Colorado, UCB-0311, Boulder, CO 80309-0311.
E-mail: fasullo@monsoon.colorado.edu

Parthasarathy 1981; Rasmusson and Carpenter 1983; Shukla and Paolino 1983; Parthasarathy and Pant 1985; Shukla 1987; Webster and Yang 1992; Krishnamurthy and Goswami 2000).

Early attempts to translate theories of monsoon–ENSO coupling into skillful predictive relationships for monsoon precipitation were largely unsuccessful due to the lack of significant persistence of SST anomalies through boreal spring and, thus, sufficient forecasting lead time (Normand 1953; Webster and Yang 1992; Webster et al. 1998). Also, during some decades, the monsoon–ENSO correlation has been weak (Troup 1965; Torrence and Webster 1999) and little is known about the physical mechanisms that induce low-frequency variability in the monsoon–ENSO relationship. Today, with the anticipation of techniques that may allow for skillful ENSO forecasts extending over several seasons (e.g., Penland and Magorian 1993; Chen et al. 1995), there is renewed interest in deciphering the monsoon–ENSO relationship.

In concert with a renewed interest in the monsoon–ENSO relationship, the actual correlation between the two systems has languished in recent decades. Figure 1 shows decadal variability in the monsoon and ENSO for each decade from 1870 to the present. Strong and weak monsoon seasons are determined as positive and negative anomalies in All India Rainfall (AIR) greater than 10%, respectively. A variety of estimates are used to identify ENSO events. A seasonal classification of ENSO events is used by the Climate Prediction Center (CPC) from 1950 onward. Also, JJAS anomalies in the Global Sea Ice and Sea Surface Temperature dataset (GISST; Rayner et al. 1996) fields >0.7°C can be used to identify cold (La Niña) and warm (El Niño) ENSO phases. A third method, that of Kiladis and Diaz (1989), identifies ENSO status for the entire year. Because SST anomalies during ENSO events do not always experience the same phase relationship with the annual cycle and because the identification methods use somewhat different methodologies, the number of ENSO events identified by the various techniques disagrees somewhat. Notwithstanding such differences, Fig. 1 reveals several interesting features of ENSO, the monsoon, and their relationship including the following:

- The number of ENSO events active in JJAS (Fig. 1a) was lowest in the 1870s and 1940s, was moderate during the early twentieth century, and was large in the late twentieth century (e.g., Torrence and Webster 1999; Elliot and Angell 1988; Meehl 1987).
- Anomalous monsoons (Fig. 1b) were frequent from the 1890s to the 1910s and again from the 1940s to the 1980s.
- Relatively few anomalous monsoon seasons occurred (two or less) during decades in which the number of anomalous monsoons accompanying ENSO was small (the 1880s, 1920s, 1930s, and 1990s) while the number of ENSO events during such decades remains modest or large (two to eight). Most recently, only a single anomalous monsoon season occurred during the 1990s despite the presence of several ENSO events.
- The number of anomalous monsoons occurring during ENSO events has changed considerably over the past century. In the 1890s, 1910s, 1970s, and 1980s, multiple anomalous monsoon seasons occurred during ENSO events while during most other decades, less than two anomalous monsoon seasons occurred during ENSO events. Only in the 1880s, 1920s, and 1990s did an anomalous monsoon fail to accompany an ENSO event (e.g., Sikka 1999).

Figure 1 highlights the fact that if predictive skill in the Niño-3 region (5°S–5°N, 90°–150°W) is to be translated into useful monsoon forecasting, the low-frequency variability in the monsoon–ENSO relationship must be understood. In particular, the factors distinguishing ENSO events in which the monsoon is anomalous from those in which the monsoon is normal are central to the coupling's intermittency. The relationships between decadal variations in the Tropics and the monsoon–ENSO association are only beginning to be explored. A basinwide shift in the Pacific Ocean SST distribution during the mid 1970s has been identified (e.g., Trenberth and Hurrell 1994; Mantua et al. 1997); however, its relationship to the monsoon–ENSO coupling is unclear. A negative correlation between the magnitude of monsoon rainfall and the standard deviation of SST in the eastern Pacific over the past century has also been identified and it is speculated that the systems may both be part of a common mode of decadal variability (Krishnamurthy and Goswami 2000). However, the relationship between the decadal mode and low-frequency shifts in the interannual monsoon–ENSO relationship is not strong.

There remain, thus, the following questions regarding the decadal variability of the monsoon–ENSO relationship:

- What are the physical processes that communicate the coupling between ENSO and the monsoon?
- How do the physical processes differ, or how are they modulated, between periods in which the monsoon–ENSO relationship is strong and periods in which it is weak?
- Do these differences offer clues to the role of the coupled system in modulating the monsoon?

The aim of this paper is to sort out the relationships between the extremes of ENSO (i.e., El Niño and La Niña), anomalies in the monsoon, and their connective circulations. As the lateral and transverse heating gradients that drive the monsoon are strongly tied to moist processes (Webster 1994), we emphasize the hydrologic cycle as a new basis for analysis.

2. Data and method

The National Centers for Environmental Prediction–National Center for Atmospheric Research (NCEP–

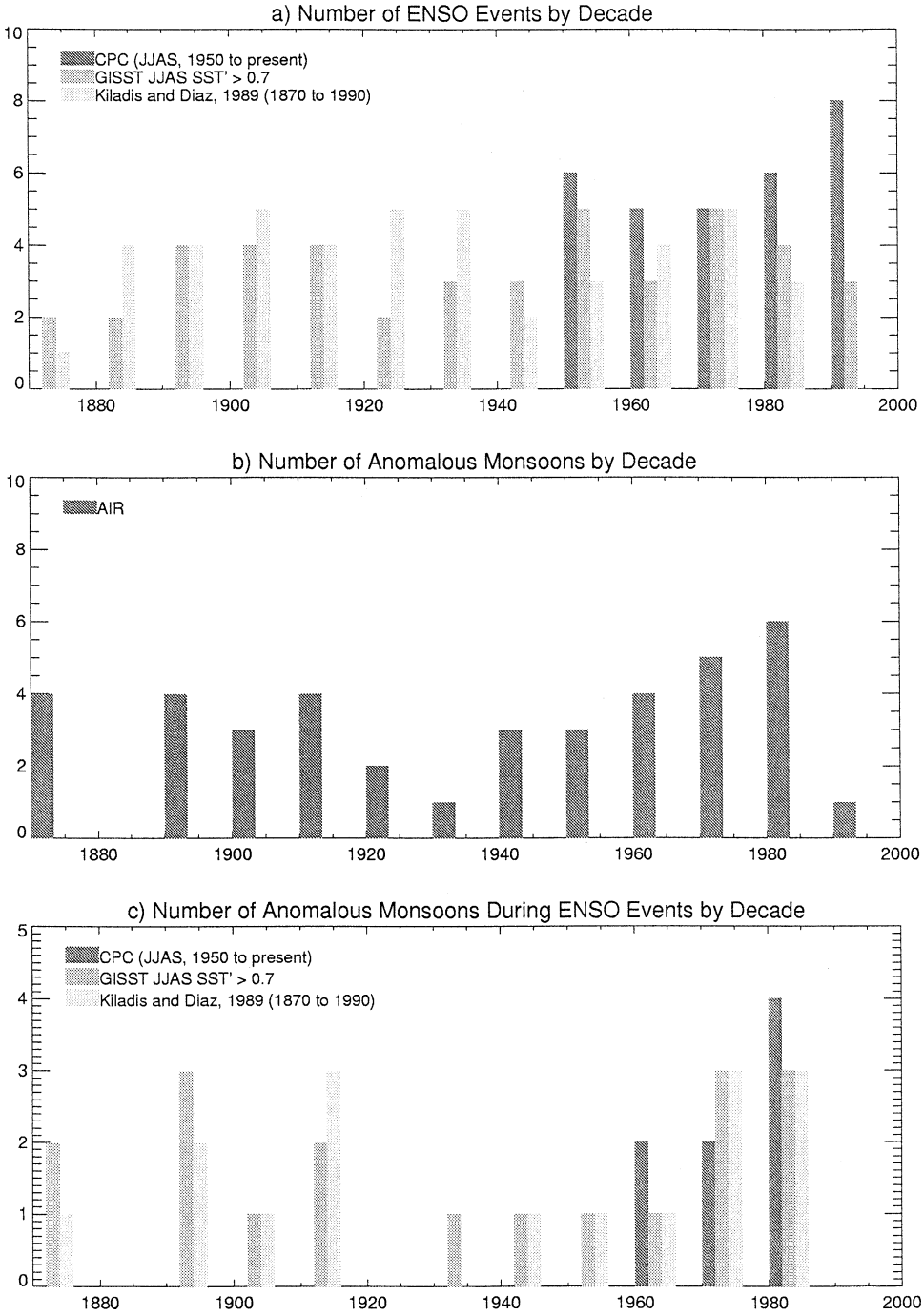

FIG. 1. (a) The number of ENSO events per decade identified by the CPC, Niño-3 GISST anomalies greater than 0.7°C, and Kiladis and Diaz (1989). (b) The total number of strong and weak monsoon seasons per decade as identified by 10% anomalies in AIR. (c) The number of anomalous monsoon seasons to accompany ENSO events per decade based on the monsoon identification in (b) and the three methods of ENSO identification in (a).

NCAR) reanalyses from 1950 to 2000 (Kalnay et al. 1996; Kistler et al. 2001) are used to estimate variability in the hydrologic cycle. The reanalyses incorporate global rawinsonde data, Comprehensive Ocean–Atmosphere Data Set (COADS) surface marine data, and surface land synoptic data through much the study's analysis period (1950–present). Satellite sounder data is also available from the Television Infrared Observational Satellite (TIROS) Operational Vertical Sounder (TOVS) and Satellite Infrared Radiation Spectrometer (SIRS)

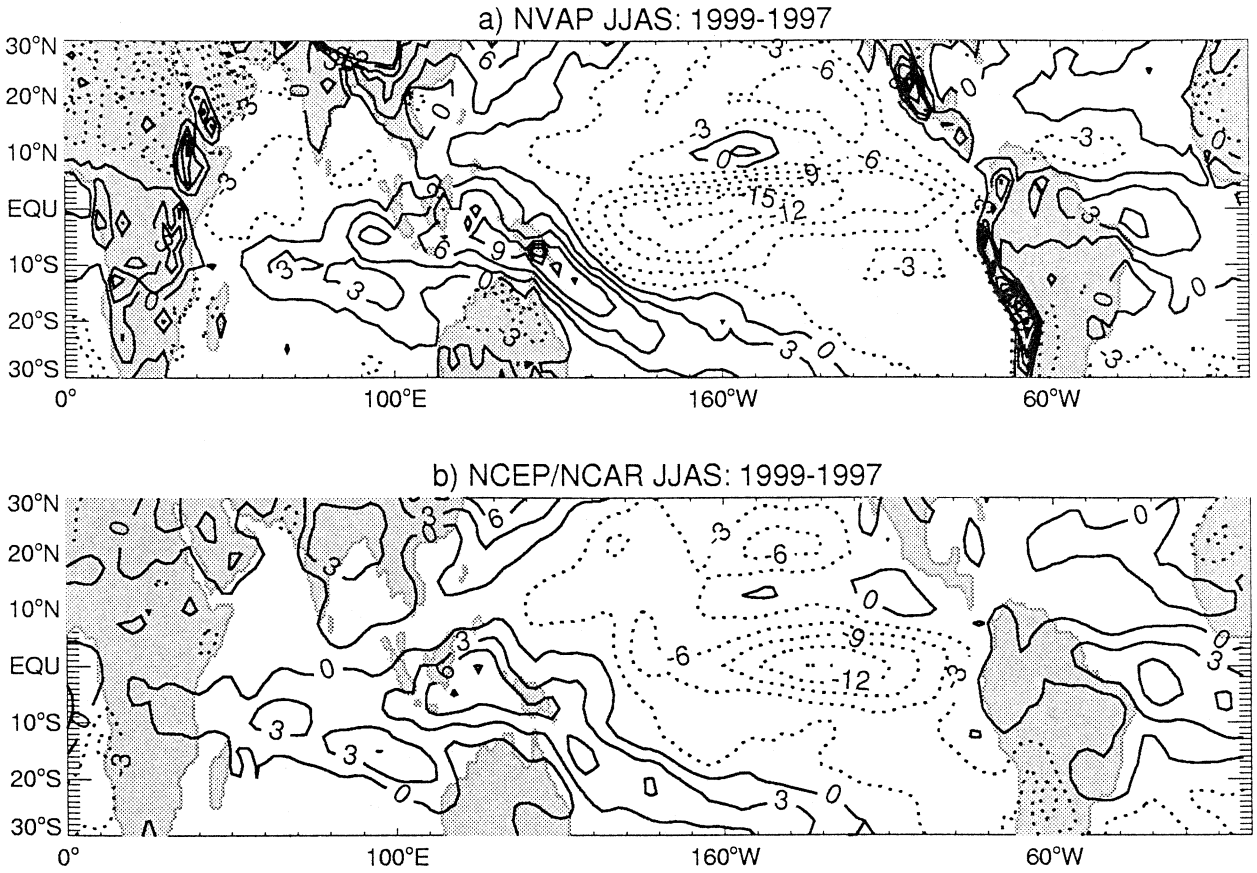

FIG. 2. The difference between atmospheric precipitable water estimates for JJAS of 1999 minus 1997 from (a) NVAP and the (b) NCEP–NCAR reanalysis.

sounders through most of the later part of the analysis period (1979–present). Total vertically integrated moisture transport (VIMT) is calculated from the reanalysis humidity and wind fields at each pressure level and 6-h forecast interval. Sea level pressure fields will also be used. Class A fields of the reanalysis, such as winds and sea level pressure, and class B fields, such as humidity, are strongly and moderately influenced by assimilated data, respectively. Winds and sea level pressure are therefore among the most reliable reanalysis fields. Since the reanalysis estimates of humidity are also strongly influenced by the model, a comparison of total atmospheric precipitable water difference with data from the National Aeronautics and Space Administration's (NASA's) Water Vapor Project (NVAP; Randel et al. 1996) for recent ENSO events are shown in Fig. 2. The difference fields show both similarities and differences. In both panels, negative differences, indicating drier conditions for La Niña than El Niño, span the equatorial Pacific Ocean and northern Indian Ocean while positive differences cover a region at 10°S spanning most of the Indian Ocean, Australia, and farther south along the southwestern Pacific Ocean. Positive differences are also apparent over much of Southeast Asia. Though magnitudes of the differences agree well between the datasets, the location of the maximum difference in the Pacific Ocean as represented by the reanalysis is displaced considerably eastward from that in satellite retrievals. Also, the magnitudes of differences in the Arabian Sea are slightly too weak in the reanalysis as compared to those in the retrievals. Nonetheless, the form and magnitude of precipitable water differences as shown by satellite are in most locations, well represented by the reanalysis.

To compile composites, both anomalous monsoon seasons and ENSO events are identified. Strong and weak monsoon seasons are determined by 10% excesses and deficits in the AIR during JJAS, respectively. Because concurrent SST anomalies are believed to be central to the monsoon–ENSO coupling, a method of identifying ENSO events while considering season, similar to that applied to GISST data in Fig. 1, is used. ENSO events are gauged from Reynolds (Reynolds and Smith 1994) and reconstructed Reynolds (Smith et al. 1996) SST anomalies in the Niño-3 region of greater than 0.7°C when averaged over JJAS. Anomalies have been computed by removing the climatological monthly means from the data. Table 1 summarizes the years in which anomalous monsoon seasons and ENSO events are identified. In all, 19 ENSO events are found with

TABLE 1. Years of identified ENSO events (see text). ENSO events associated with strong and weak monsoon seasons are shown in bold.

Cold events	Warm events
1954	1953
1955	1957
1970	1963
1973	**1965**
1975	1969
1988	**1972**
1999	1976
	1982
	1983
	1987
	1991
	1997

12 classified as ''warm'' (i.e., El Niño) and 7 classified as ''cold'' (i.e., La Niña). At least three ENSO events occur during all decades and less than half of the ENSO events are associated with anomalous monsoons.

Linear composites of hydrologic fields for both warm and cold events are then created. While the seasonal identification method chosen here is believed to be more relevant to the monsoon–ENSO coupling than classifications that identify ENSO by year alone, as it reflects Niño-3 conditions during the monsoon season, the principal findings of the analysis are not significantly altered by considering alternative ENSO classifications. The ENSO events are stratified into two groups: one representing La Niña and, El Niño years associated with ENSO–anomalous monsoons (EAM) and one associated with ENSO–normal monsoons (ENM). Together the EAM and ENM groups will be used to compare and contrast hydrologic fields during periods of strong and weak coupling, respectively.

3. The mean monsoon hydrologic cycle

The hydrological cycle can be most generally described by the VIMT into and out of a region, and the precipitation (P), evaporation (E), and precipitable water (PW) within the region. Vertically integrated moisture transport is defined as

$$\text{VIMT} = \int_{\text{surface}}^{300\text{ mb}} q \cdot \mathbf{U}\ (\partial p),$$

where q is the specific humidity and $\mathbf{U}$ is the wind vector. Above 300 mb, specific humidity amounts are poorly known and are therefore not part of the reanalysis (Kalnay et al. 1996). However, above 300 mb, specific humidity in the Tropics is at least two orders of magnitude smaller than near the surface and moisture transports are therefore of negligible influence to the calculation of VIMT. Figures 3a,b, and c show the climatological mean JJAS precipitation minus evaporation ($P - E$), VIMT, and VIMT integrated across key boundaries in the Indian and Pacific Oceans, respectively. The boundaries are chosen to draw distinctions between

- the Northern and Southern Hemisphere;
- the western Pacific Ocean, Indonesia, and the eastern and western Indian Ocean regions; and,
- the near-equatorial and monsoonal regions of deep convection associated with the local Hadley circulation which has been identified as key in the monsoon–ENSO interaction (e.g., Goswami 1998).

The largest zonal VIMT occurs in the westerly flow over India, the Bay of Bengal, and Southeast Asia, and the easterly flow in the southern Indian Ocean and central Pacific Ocean. Interhemispheric VIMT is large in the western Indian Ocean and near Indonesia. Together, these principal circulations constitute two cross-equatorial exchanges of moisture that couple regions of substantial Southern Hemisphere divergence with regions of strong Northern Hemisphere convergence associated with the major centers of monsoonal convection (Wang and Fan 1999; Murakami et al. 1999). In the first circulation, the Somali jet, a feature that is key in the exchange of mass and moisture between hemispheres (e.g., Findlater 1969; Murakami et al. 1999), carries moisture from the divergent regions of the southern Indian Ocean northward into the Arabian Sea where VIMT increases due to local moisture divergence ($P < E$). Southerly VIMT in the Arabian Sea is less than half as strong at 12°N as at the equator but additional divergence and northerly VIMT into the northern Arabian Sea contribute to westerly VIMT of 340×10^6 kg s^{-1} toward the convergent ($P > E$) deep convective regions near India and the Bay of Bengal. Also, large southerly VIMT into the Indian and Bay of Bengal regions contributes 222×10^6 kg s^{-1}. Export from the Bay of Bengal region includes southerly VIMT of 165×10^6 kg s^{-1} and westerly VIMT of 193×10^6 kg s^{-1}. A second circulation is supplied by moisture divergence in the southern Pacific Ocean subtropics and the Indian Ocean northwest of Australia. Southerly VIMT centered about 120°E at 12°N carries 396×10^6 kg s^{-1} of moisture toward the strongly convergent deep convective regions near Southeast Asia, the South China Sea, and the Philippines. Easterly VIMT from the Pacific Ocean north of the equator contributes only 226×10^6 kg s^{-1} to convergence west of 140°E as compared to westerly VIMT across 100°E which is a factor of 2 larger, and southerly VIMT at the equator of 260×10^6 kg s^{-1}. As the focus of the current study lies in understanding ENSO's relationship with rainfall over India, the hydrologic cycle in the Indian and Bay of Bengal regions (12°–25°N, 70°–100°E) and the hydrologic anomalies associated with low-frequency variability in the monsoon–ENSO relationship will now be examined.

4. Monsoon hydrologic cycle and differences between ENSO phases

Figure 4 shows differences in SST (Fig. 4a), VIMT (Fig. 4b), and boundary-integrated VIMT (Fig. 4c)

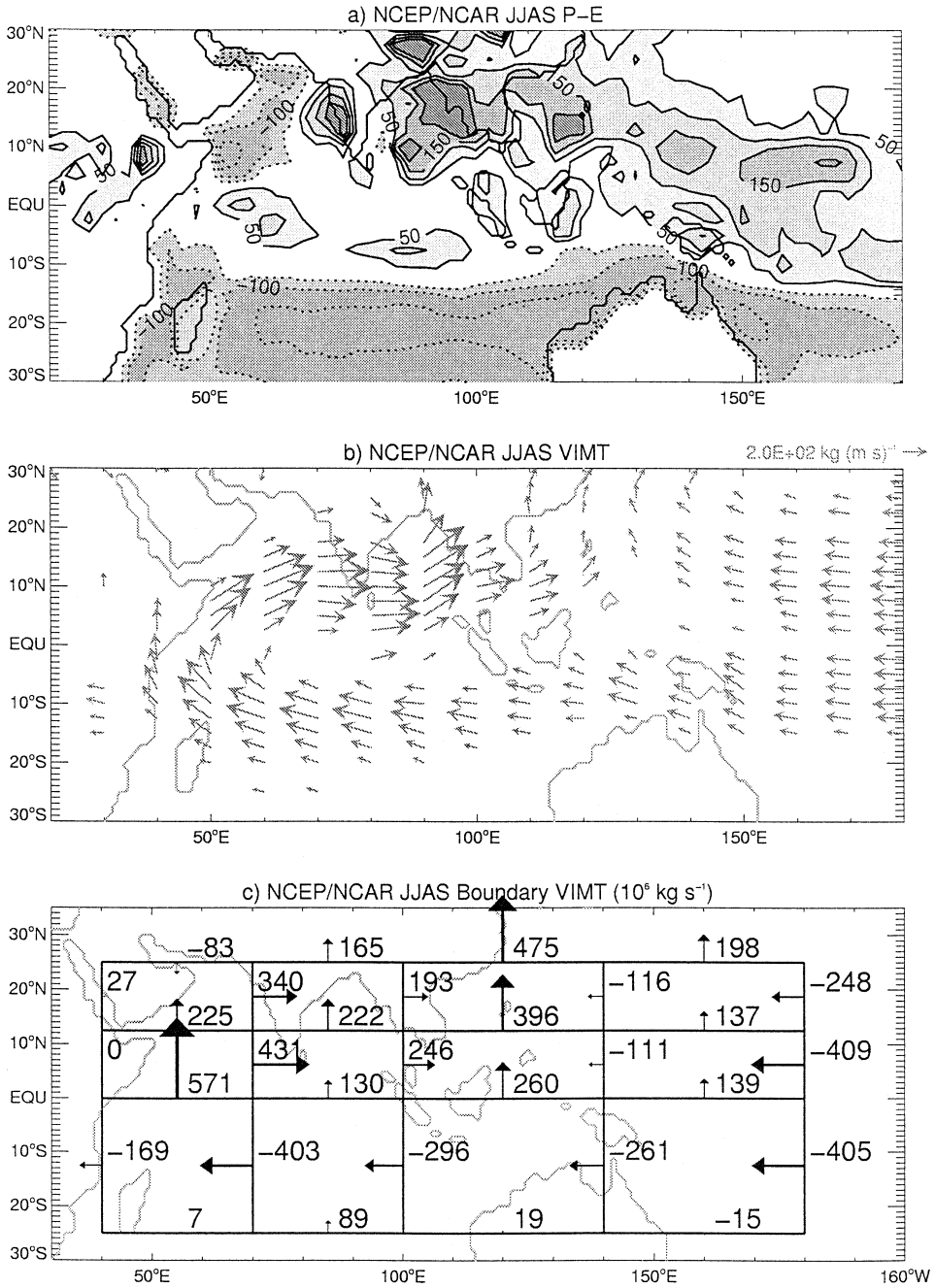

FIG. 3. The mean monsoon hydrologic cycle during JJAS from 1958 to 2000 as depicted by the NCEP–NCAR reanalysis. Shown are (a) $P - E$ (shading) in units of latent energy (W m^{-2}), (b) VIMT in units of kg m^{-1} s^{-1}, and (c) integrated transports across key boundaries (see text) in the Indian and Pacific Oceans.

between La Niña and El Niño periods for JJAS from 1950 to 2000. Large differences exist in the hydrologic fields between these ENSO extremes. As expected, SST is cooler throughout the eastern Pacific Ocean during La Niña events and warmer in the western equatorial and western subtropical Pacific Ocean, and eastern Indian Ocean than during El Niño years. During La Niña events, easterly VIMT is enhanced across the date line and 140°E relative to warm events. As VIMT is strongly biased toward the low-level flow, the VIMT anomalies are consistent with the enhancement of the Pacific Ocean trade winds associated with a westward-displaced and strengthened Walker circulation during La Niña and an eastward-displaced and weakened circulation during El Niño (e.g., Rasmusson and Carpenter 1982). However, at 100°E,

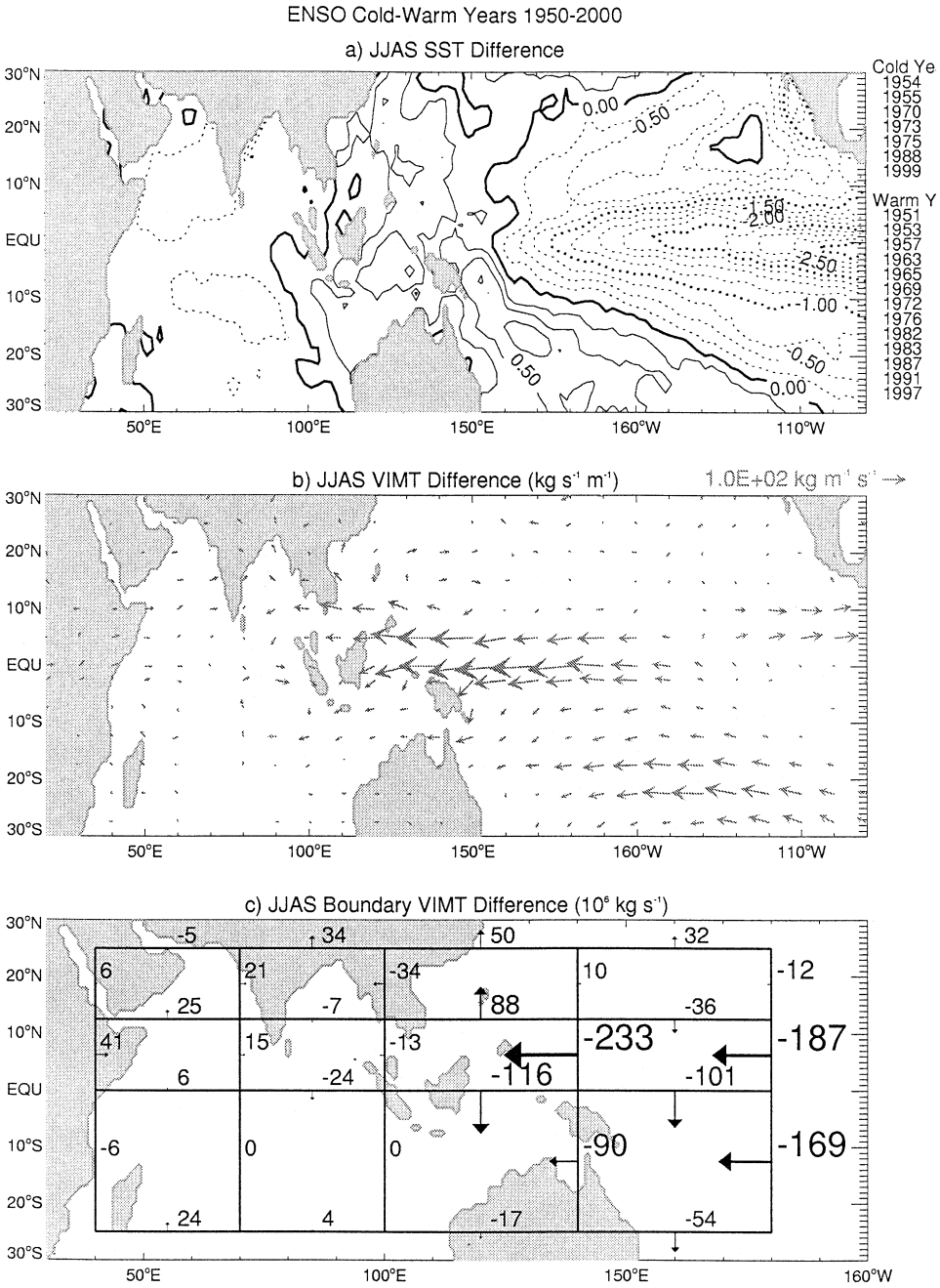

FIG. 4. The composite difference between La Niña and El Niño events during JJAS in (a) reconstructed Reynolds SST, (b) VIMT, and (c) boundary integrated VIMT based on events from 1958 to 2000. Large and very large fonts for boundary integrated VIMT denote statistical significance from the climatological JJAS distribution at the 90% and 95% levels, respectively. Statistical significance is established through the Monte Carlo technique.

anomalous zonal VIMT has diminished and contributes only modestly to the variability in moisture convergence in the Indian Ocean. In fact, on average, VIMT anomalies in the Indian Ocean associated with ENSO are very small relative to those in the Pacific Ocean. Moreover, moisture convergence over India and the Bay of Bengal region (12°–25°N, 70°–100°E) is only modestly greater (14×10^6 kg s^{-1}) during La Niña years than during El Niño years. Westerly VIMT from the Arabian Sea associated with the transverse monsoon (Webster 1994) contributes a modest amount to variability in moisture convergence near India (21×10^6 kg s^{-1}). Differences in VIMT into the Arabian Sea include variations in the Somali jet (6×10^6 kg s^{-1}),

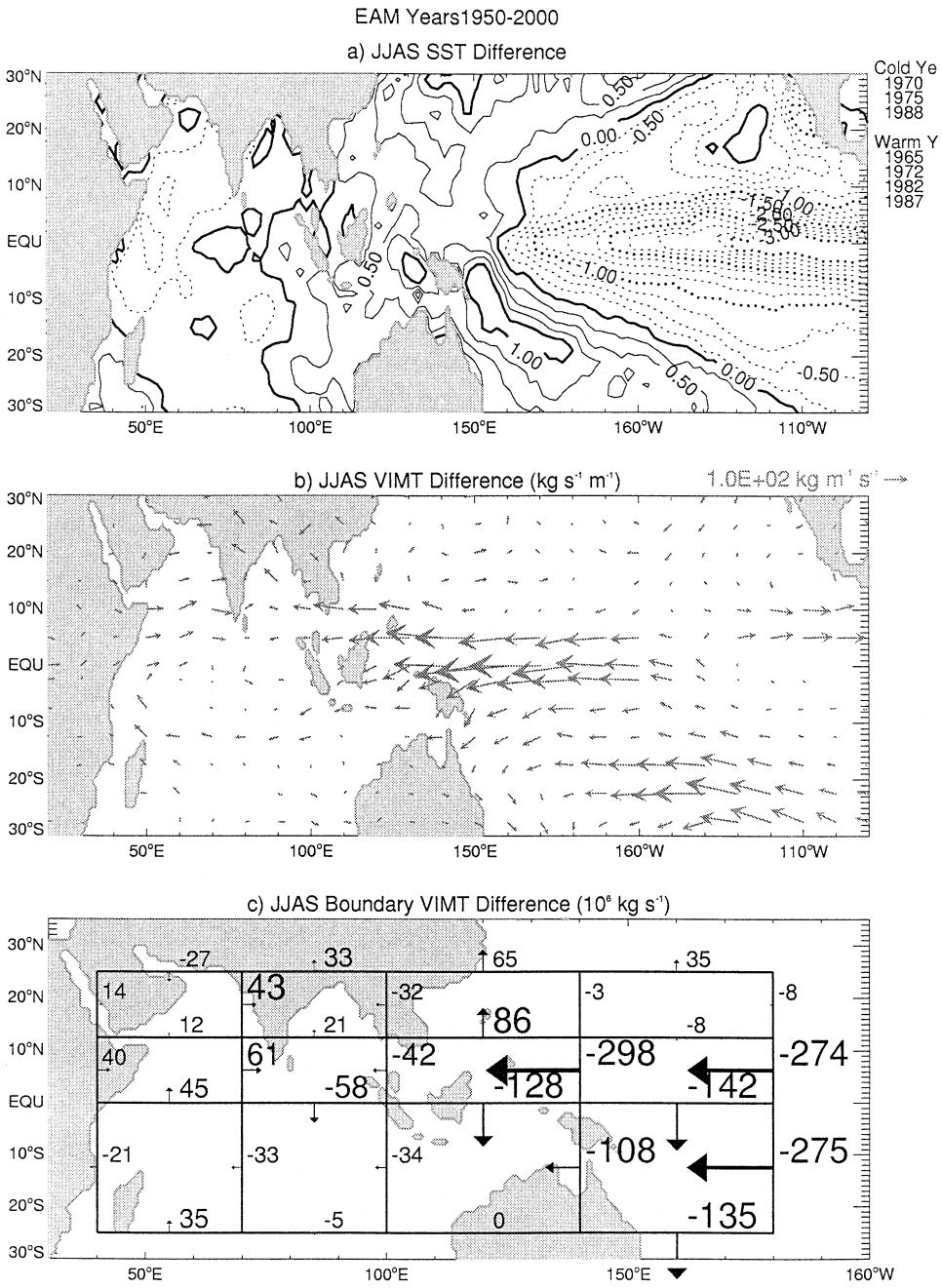

FIG. 5. As in Fig. 4 but for the difference in ENSO extremes occurring concurrently with anomalous monsoons (EAM periods).

southerly VIMT across 12°N (25×10^6 kg s^{-1}), and westerly VIMT from equatorial Africa (41×10^6 kg s^{-1}) between ENSO phases. Meanwhile, convergence of moisture south of India and the Bay of Bengal regions (0°–12°N, 70°–100°E) is 11×10^6 kg s^{-1} stronger during La Niña years than during El Niño years. Also, westerly transports across 100°E from the equator to 12°N are slightly weaker during La Niña years than El Niño years (13×10^6 kg s^{-1}). In addition to VIMT anomalies from the Pacific Ocean, the processes that modify VIMT into the Arabian Sea and eastward toward India are thus importantly involved in the changes in moisture convergence in the India and Bay of Bengal regions that occur between ENSO phases. As such, the pattern of VIMT anomalies does not simply result from enhanced VIMT associated with anomalies in the Pacific trade winds. As a further stratification, we now examine the hydrologic cycle in those years where the extremes of

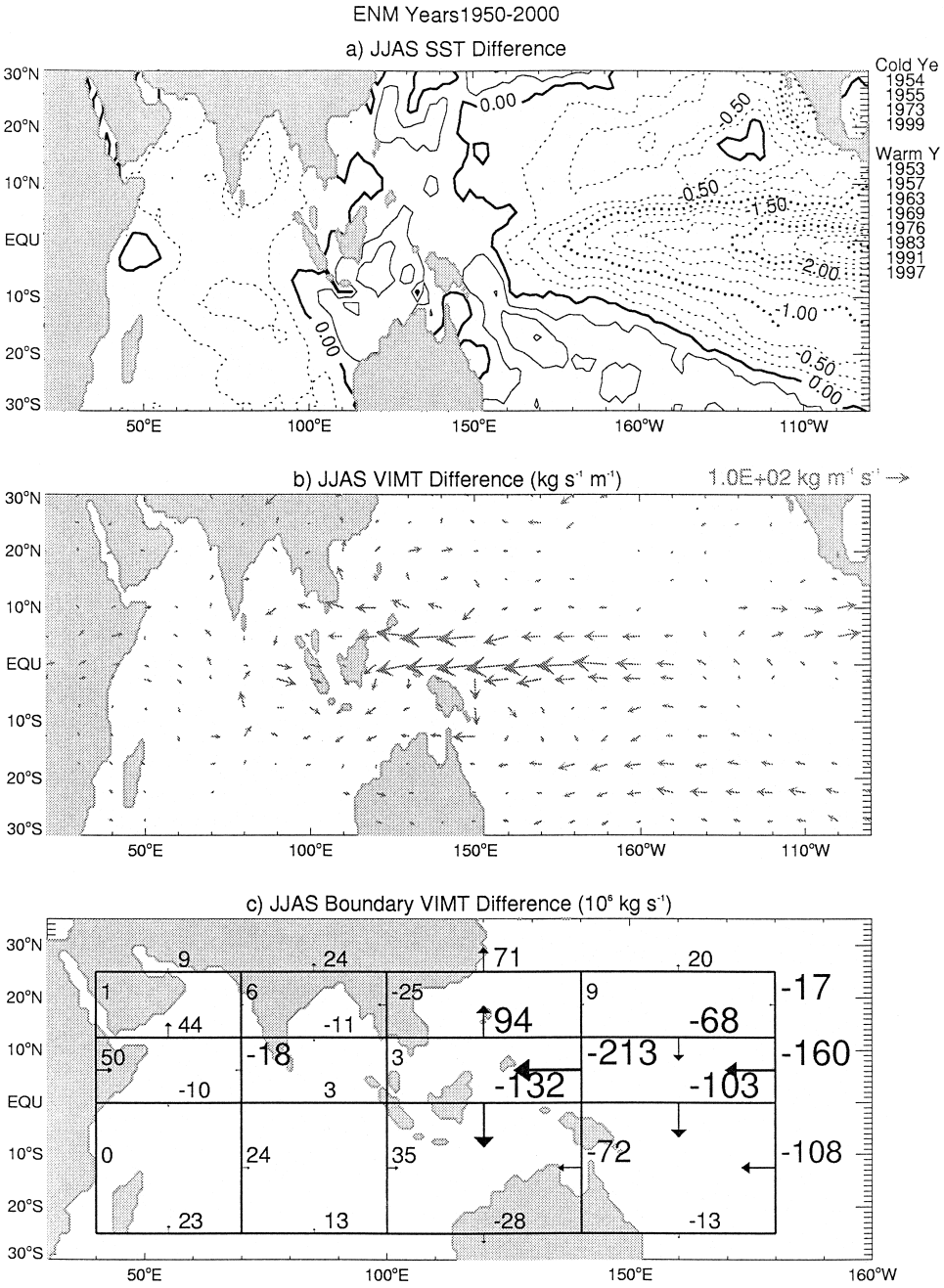

FIG. 6. As in Fig. 4 but for the difference in ENSO extremes occurring in the absence of anomalous monsoons (ENM periods).

ENSO are associated with extremes in monsoonal rainfall over India as compared to ENSO years in which Indian rainfall is near normal.

5. Differences in the hydrologic cycle between years of strong and weak monsoon–ENSO coupling

Figures 5 and 6 show the difference in VIMT and SST between La Niña and El Niño years associated with anomalous monsoons (Fig. 5) and years associated with normal monsoons (Fig. 6), or, respectively, EAM and ENM years, as defined in section 2. Many of the characteristics of the mean ENSO pattern (Fig. 4) exist irrespective of the monsoon strength. For example, in both EAM and ENM years relatively cool SST predominates in La Niña throughout the eastern Pacific Ocean and central Indian Ocean while warm SST exists in the western Pacific Ocean and eastern Indian Ocean. In both categorizations, anomalous VIMT during La Niña is easterly across the central and western

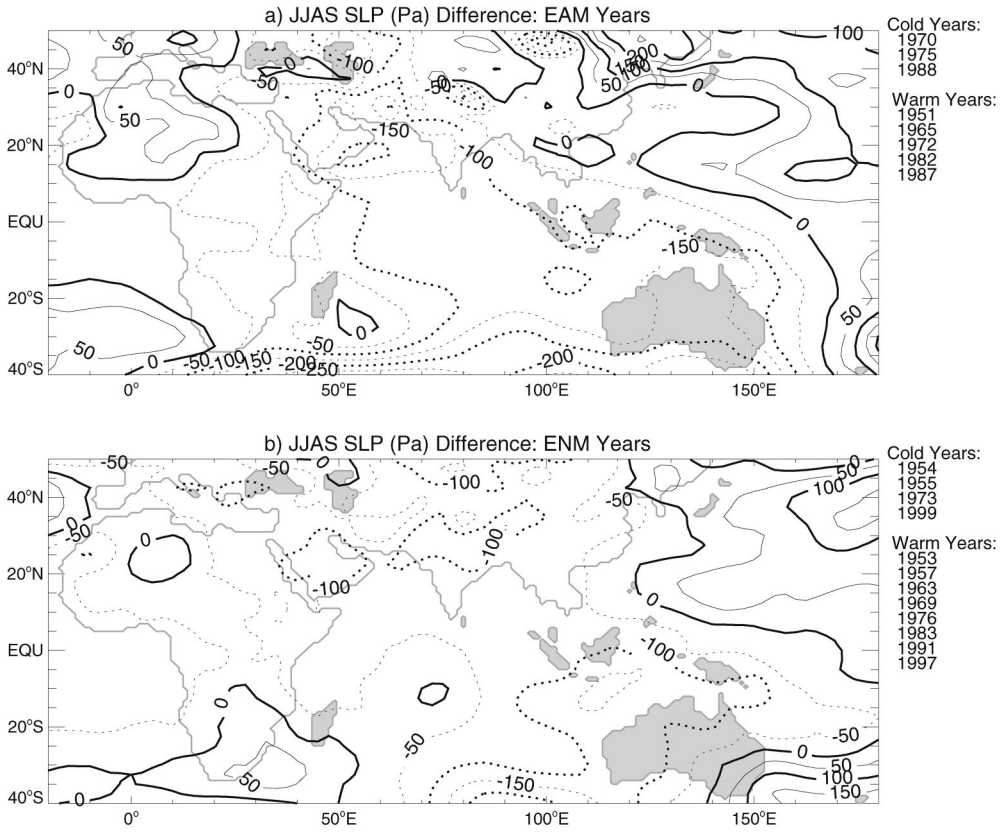

FIG. 7. The mean sea level pressure distribution difference (Pa) between cold and warm phases of ENSO for (a) EAM seasons and (b) ENM seasons.

Pacific Oceans, southerly across the Philippines, and northerly across Indonesia relative to El Niño years. Also, differences in easterly VIMT into India and the Bay of Bengal regions are substantively similar in each categorization. However, important distinctions also exist between EAM and ENM periods. SST anomalies in both the eastern and western Pacific Ocean are larger during EAM years than ENM years, as are VIMT differences, in both the Pacific and Indian Oceans. Additionally, substantial VIMT differences eastward from the Arabian Sea and northward through the Somali jet occur during EAM years while the differences are near zero for ENM years. Differences in meridional VIMT into India and the Bay of Bengal regions are southerly during EAM years but are northerly during ENM periods. Thus, the different manner in which moisture convergence variability occurs in India and the Bay of Bengal regions during ENSO events, as a function of monsoon strength, results primarily from variability in VIMT from the Arabian Sea and equatorial Indian Ocean rather than from the variability in easterly VIMT crossing 100°E, which is associated with the trade winds.

Other significant changes in ENSO-related VIMT differences are also apparent. Across 100°E between the equator and 12°N, VIMT differences are strong and easterly during EAM years but are near zero during ENM years. Furthermore, in EAM years, anomalies are also substantially larger throughout the equatorial and southern Pacific Ocean than in ENM years. The larger VIMT in the southern Pacific Ocean is also associated with a larger zonal gradient in SST.

Figure 7 shows the SLP difference field from EAM (Fig. 7a) and ENM (Fig. 7b) years. While the difference fields in the western Pacific and eastern Indian Oceans are generally similar, there are some important differences. For both composites, SLP in the western Indian Ocean during La Niña events is lower than for El Niño events. During EAM years, however, the difference is -175 Pa (-1.75 mb) to -200 Pa (-2 mb) while during ENM years, the difference is only half as large (-75 Pa or -0.75 mb). During EAM years, anomalously low pressure in the northern Arabian Sea enhances the regional cyclonic low-level circulation and thus apparently acts to increase westerly VIMT across the Arabian Sea and into India as shown in Figs. 5b and 5c. The reduction of differences in SLP gradients in the western Indian Ocean during ENM years is thus consistent with reduced differences in VIMT into India and the Bay of Bengal regions (Figs. 6b,c) and the consequent reduction in moisture convergence there. Mechanisms determining SLP and VIMT in the Arabian Sea during ENSO

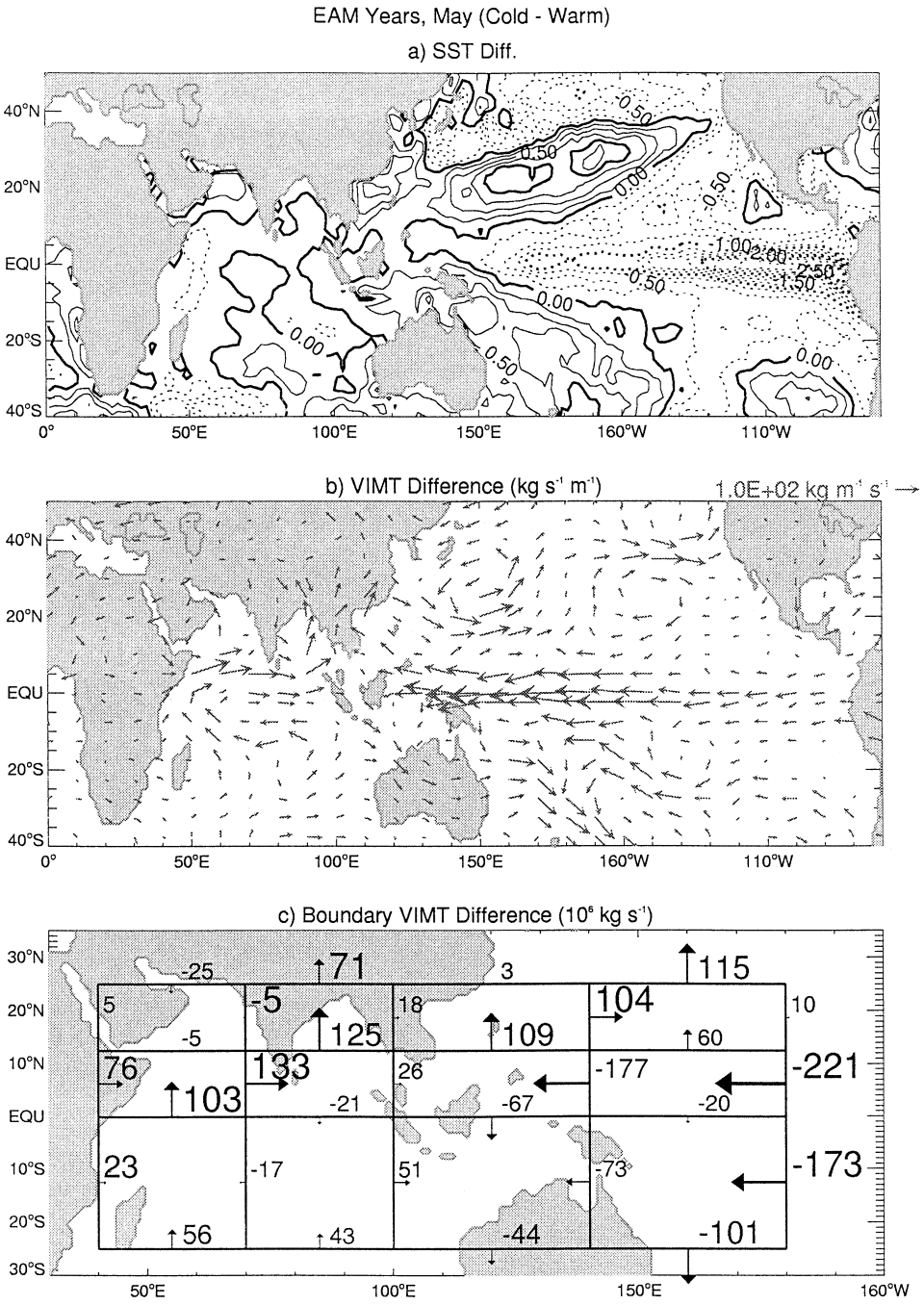

FIG. 8. The difference in (a) SST (contours), (b) VIMT, and (c) boundary integrated VIMT for May ENSO events preceding EAM periods. Large and very large fonts for integrated transports denote statistical significance from the climatological distribution of May conditions at the 90% and 95% levels, respectively.

events are thus identified to be key components of the intermittency in the monsoon–ENSO relationship.

6. Discussion and conclusions

The analysis has attempted to identify variations in the monsoon hydrologic cycle associated with El Niño and La Niña. Additionally, differences in hydrologic variability based on the strength of the monsoon have been compared to establish the major differences between monsoon seasons in which the monsoon–ENSO coupling is strong (EAM periods) and seasons in which it is weak (ENM periods). Some key conclusions can be made about the nature of the monsoon–ENSO in-

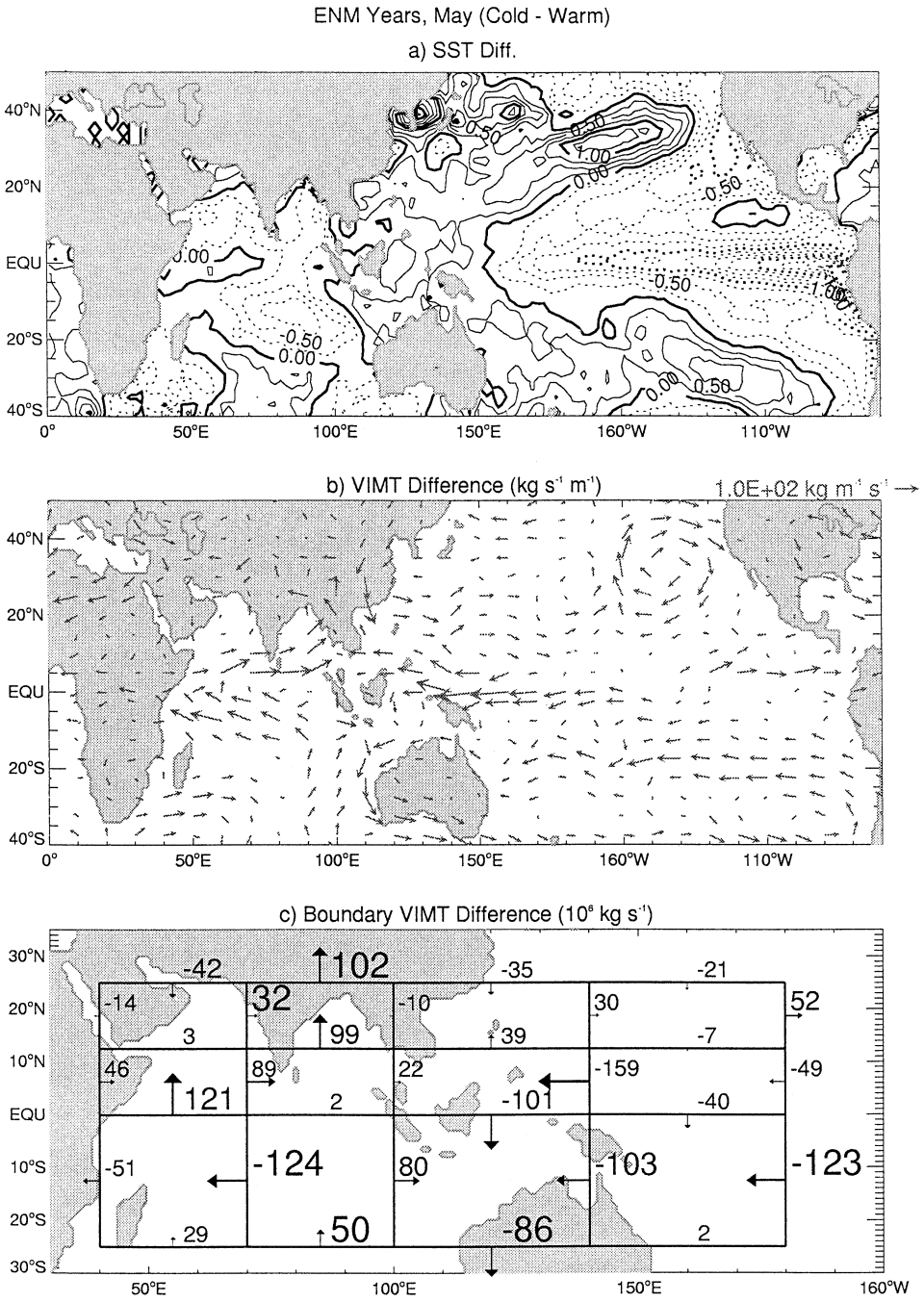

FIG. 9. As in Fig. 8 but for May of ENSO events preceding ENM periods.

teraction. First, modification of moisture convergence in India and the Bay of Bengal regions during ENSO events is due to both enhanced westerly VIMT from the Arabian Sea and anomalous easterly VIMT from the Pacific Ocean. Differences in SLP are consistent with the observed differences in VIMT in the Arabian Sea as, in general, lower surface pressure exists in the northern Arabian Sea during La Niña events than during El Niño events. The cyclonic circulation associated with the SLP difference minimum in the Arabian Sea is thus located on the northern fringe of westerly VIMT into India and serves to strengthen westerly flow into India.

There exists little difference in easterly VIMT anomalies from the Pacific Ocean between ENM and EAM years. However, large differences between ENSO phases exist in SLP and VIMT in the Arabian Sea during EAM years while, during ENM years, the differences are relatively small. The net impact of the SLP and VIMT

differences is to increase the variability in moisture convergence over India during EAM years relative to ENM years. Moreover, changes are observed throughout the monsoon gyre with VIMT differences in the Somali jet and across the equator from 70° to 100°E being large during EAM years but small for ENM years. Additionally, large easterly differences in VIMT exist in the southern Pacific Ocean during EAM years while small differences occur during ENM years.

Discerning the causal relationships between the difference fields in Figs. 4–7 remains a key science objective. In particular, it is unclear if the larger SST differences in the eastern Pacific Ocean during EAM periods cause the difference in monsoon intensity or result from it. While it is not possible to deduce fully the causal relationships between the monsoon and ENSO at this time, some insight may be gained by examining the anomalies that exist in the month prior to the monsoon onset. To this end, Figs. 8 and 9 show the differences between VIMT and SST during May for EAM and ENM periods, respectively. A number of features of the difference fields stand out. First, peak SST differences in the eastern Pacific Ocean during May are similar in magnitude for ENSO events during ENM years and during EAM years at about 2.5°C. The stronger monsoon coupling with ENSO that occurs during EAM years thus does not appear to result from stronger SST anomalies in the eastern Pacific Ocean during May. However, SST anomalies in the subtropical central and western Pacific Ocean are somewhat stronger during May of EAM years (0.5°–1.0°C) than ENM years (0°–0.25°C). Moreover, VIMT anomalies in the central and western Pacific Ocean associated with the zonal SST gradient are considerably stronger for the May of the EAM years than the May of ENM years. Also both the zonal VIMT in the central Indian Ocean and southerly transport into India are considerably stronger for EAM years relative to ENM years. The anomalies occurring in May, in fact, are similar in form to the subsequent differences that are observed during the monsoon season (JJAS) with stronger trade wind anomalies, westerly VIMT anomalies in equatorial Indian Ocean, and easterly VIMT anomalies in the southern Pacific Ocean occurring in May prior to the EAM periods. The larger VIMT differences observed in both the Indian and Pacific Oceans during JJAS of EAM years are therefore not simply the result of the monsoon seasons that they precede or the magnitude of the ENSO events in May, but rather, are associated with details of the premonsoon environment during boreal spring and characteristics of the emerging ENSO events across the Pacific Ocean.

Many questions remain. First, there is a need to confirm the results found here using alternative datasets such as the European Centre for Medium-Range Weather Forecasts (ECMWF) 40-yr reanalysis. Moreover, in identifying VIMT in the Arabian Sea as the dominant contributor to the differences in moisture convergence variability in India and the Bay of Bengal between EAM and ENM years, this study has developed a rationale to examine the processes that alter the SLP and VIMT in the northern Arabian Sea on interannual and decadal timescales. Also, the importance of the SST gradient and its associated VIMT anomalies in the subtropical western and central Pacific Ocean as parts of the monsoon–ENSO coupling has been highlighted. Modeling efforts that focus on the interplay between these essential components of the monsoon system hold the promise of distilling the multiple and complex interactions between the Indian monsoon and ENSO systems.

Acknowledgments. This work was completed under the support of NSF Grant ATM-9526030 and DOE Grant DE-FG03-94ER61770.

REFERENCES

Barnett, T. P., 1983: Interaction of the monsoon and Pacific trade wind system at interannual time scales. Part I: The equatorial zone. *Mon. Wea. Rev.*, **111,** 756–773.

——, 1984: Interaction of the monsoon and Pacific trade wind system at interannual time scales. Part III: A partial anatomy of the Southern Oscillation. *Mon. Wea. Rev.*, **112,** 2388–2400.

Chen, D., S. E. Zebiak, A. J. Busalacchi, and M. A. Cane, 1995: An improved procedure for El Niño forecasting—Implications for predictability. *Science,* **269,** 1699–1902.

Elliot, W. P., and J. K. Angell, 1988: Evidence for changes in Southern Oscillation relationships during the last 100 years. *J. Climate,* **1,** 729–737.

Findlater, J., 1969: Interhemispheric transport of air in the lower troposphere over the western Indian Ocean. *Quart. J. Roy. Meteor. Soc.,* **95,** 400–403.

Gershunov, A., and T. P. Barnett, 1998: Interdecadal modulation of ENSO teleconnections. *Bull. Amer. Meteor. Soc.,* **79,** 2715–2725.

Goswami, B. N., 1998: Interannual variations of Indian summer monsoon in a GCM: External conditions versus internal feedbacks. *J. Climate,* **11,** 501–522.

Ju, J., and J. Slingo, 1995: The Asian summer monsoon and ENSO. *Quart. J. Roy. Meteor. Soc.,* **121,** 1133–1168.

Kalnay, E., and Coauthors, 1996: The NCEP/NCAR 40-Year Reanalysis Project. *Bull. Amer. Meteor. Soc.,* **77,** 437–471.

Kiladis, G. N., and H. F. Diaz, 1989: Global climatic anomalies associated with extremes in the Southern Oscillation. *J. Climate,* **2,** 1069–1090.

Kistler, R., and Coauthors, 2001: The NCEP–NCAR 50-Year Reanalysis: Monthly Means CD-ROM and Documentation. *Bull. Amer. Meteor. Soc.,* **82,** 247–268.

Krishnamurthy, V., and B. N. Goswami, 2000: Indian Monsoon–ENSO relationship on interdecadal timescale. *J. Climate,* **13,** 579–595.

Lau, K.-M., and W. Bua, 1998: Mechanism of monsoon–Southern Oscillation coupling: Insights from GCM experiments. *Climate Dyn.,* **14,** 759–779.

——, K.-M. Kim, and S. Yang, 2000: Dynamical and boundary forcing characteristics of regional components of the Asian summer monsoon. *J. Climate,* **13,** 2461–2482.

Mantua, J. N., S. R. Hare, Y. Zhang, J. M. Wallace, and R. C. Francis, 1997: A Pacific interdecadal climate oscillation with impacts on salmon production. *Bull. Amer. Meteor. Soc.,* **78,** 1069–1080.

Meehl, G. A., 1987: The annual cycle and interannual variability in the tropical Pacific and Indian Ocean region. *Mon. Wea. Rev.,* **115,** 27–50.

Murakami, T., J. Matsumoto, and A. Yatagai, 1999: Similarities as well as differences between summer monsoons over Southeast Asia and the western North Pacific. *J. Meteor. Soc. Japan,* **77,** 887–906.

Normand, C., 1953: Monsoon seasonal forecasting. *Quart. J. Roy. Meteor. Soc.,* **79,** 463–473.

Pant, G. B., and B. Parthasarathy, 1981: Some aspects of an association between the Southern Oscillation and Indian summer monsoon. *Arch. Meteor. Geophys. Biokl.,* **29,** 245–252.

Parthasarathy, B., and G. B. Pant, 1985: Seasonal relationship between Indian summer monsoon rainfall and Southern Oscillation. *J. Climatol.,* **5,** 369–378.

Penland, C., and T. Magorian, 1993: Prediction of Niño-3 sea surface temperatures using linear inverse modeling. *J. Climate,* **6,** 1067–1076.

Randel, D. L., T. J. Greenwald, T. H. vonder Haar, G. L. Stephens, M. A. Ringerud, and C. L. Combs, 1996: A new global water vapor dataset. *Bull. Amer. Meteor. Soc.,* **77,** 1233–1254.

Rasmusson, E. M., and T. H. Carpenter, 1982: Variations in tropical sea surface temperature and surface wind fields associated with the Southern Oscillation–El Niño. *Mon. Wea. Rev.,* **110,** 354–384.

——, and ——, 1983: The relationship between eastern equatorial Pacific sea surface temperature and rainfall over India and Sri Lanka. *Mon. Wea. Rev.,* **111,** 517–528.

Rayner, N. A., E. B. Horton, D. E. Parker, C. K. Folland, and R. B. Hackett, 1996: Version 2.2 of the Global sea-ice and Sea Surface Temperature data set, 1903–1994. Climate Research Tech. Note 74 (CRTN74), Hadley Centre for Climate Prediction and Research, Met Office, Bracknell, Berkshire, United Kingdom, 21 pp.

Reynolds, R. W., and T. M. Smith, 1994: Improved global sea surface temperature analyses using optimum interpolation. *J. Climate,* **7,** 929–948.

Rodwell, M. J., and B. J. Hoskins, 2001: Subtropical anticyclones and summer monsoons. *J. Climate,* **14,** 3192–3122.

Shukla, J., 1987: Interannual variability of monsoons. *Monsoons,* J. S. Fein and P. L. Stephens, Eds., Wiley and Sons, 399–464.

——, and D. A. Paolino, 1983: The Southern Oscillation and long-range forecasting of the summer monsoon rainfall over India. *Mon. Wea. Rev.,* **111,** 1830–1837.

Sikka, D. R., 1980: Some aspects of the large scale fluctuations of summer monsoon rainfall over India in relation to fluctuations in the planetary and regional scale circulation parameters. *Proc. Ind. Acad. Sci. (Earth Planet. Sci.),* **89,** 179–195.

——, 1999: Monsoon drought in India. Joint COLA/CARE Tech. Rep. 2, 270 pp.

Smith, T. M., R. W. Reynolds, R. E. Livezey, and D. C. Stokes, 1996: Reconstruction of historical sea surface temperature using empirical orthogonal functions. *J. Climate,* **9,** 1403–1420.

Torrence, C., and P. J. Webster, 1999: Interdecadal changes in the ENSO–monsoon system. *J. Climate,* **12,** 2679–2690.

Trenberth, K. E., and J. W. Hurrell, 1994: Decadal atmosphere–ocean variations in the Pacific. *Climate Dyn.,* **9,** 303–319.

Troup, A. J., 1965: The Southern Oscillation. *Quart. J. Roy. Meteor. Soc.,* **91,** 490–506.

Walker, G. T., 1923: Correlations in seasonal variations of weather, VIII. *Memo. India Meteor. Dept.,* **24,** 75–131.

Wang, B., and Z. Fan, 1999: Choice of south Asian summer monsoon indices. *Bull. Amer. Meteor. Soc.,* **80,** 629–638.

Webster, P. J., 1994: The role of hydrological processes in ocean–atmosphere interaction. *Rev. Geophys.,* **32,** 427–476.

——, and S. Yang, 1992: Monsoon and ENSO: Selectively interactive systems. *Quart. J. Roy. Meteor. Soc.,* **118,** 877–926.

——, V. O. Magana, T. N. Palmer, J. Shukla, R. A. Tomas, M. Yanai, and T. Yasunari, 1998: Monsoons: Processes, predictability, and the prospects for prediction. *J. Geophys. Res.,* **103** (C7), 14 451–14 510.